Received: 24 November 2021 | Revised: 20 February 2023 | Accepted: 13 July 2023

DOI: 10.1002/mgg3.2253

Molecular Genetics & Genomic Medicine Open Access WILEY

CLINICAL REPORT

A novel splicing variation in *L1CAM* is responsible for recurrent fetal hydrocephalus

Tiantian He[1,2,3] | **Qiang Yao**[2,3] | **Bocheng Xu**[1,2,3] | **Mei Yang**[1,2,3] | **Jieni Jiang**[1,2,3] | **Qingqing Xiang**[1,2,3] | **Like Xiao**[1,2,3] | **Shanling Liu**[1,2,3] | **He Wang**[1,2,3] | **Xuemei Zhang**[1,2,3]

[1]Department of Medical Genetics & Prenatal Diagnosis Center, West China Second University Hospital, Sichuan University, Chengdu, China

[2]Department of Obstetrics and Gynecology, West China Second University Hospital, Sichuan University, Chengdu, China

[3]Key Laboratory of Birth Defects and Related Diseases of Women and Children (Sichuan University), Ministry of Education, Chengdu, China

Correspondence
Xuemei Zhang, Department of Medical Genetics & Prenatal Diagnosis Center, West China Second University Hospital, Sichuan University, Chengdu, China.
Email: xuemeizh001@163.com

Funding information
New Bud Fund of West China Second Hospital of Sichuan University, Grant/Award Number: KX240; Science and Technology Department of Sichuan Province of China, Grant/Award Number: 2017SZ0111

Abstract

Background: The L1 cell adhesion molecule (*L1CAM*, OMIM 308840) gene is primarily expressed in the nervous system and encodes the L1 adhesion molecule protein. Variations in *L1CAM* cause a wide spectrum of X-linked neurological disorders summarized as the L1 syndrome.

Methods: We report a 29-year-old pregnant woman who experienced multiple adverse pregnancy outcomes due to recurrent fetal hydrocephalus with an X-linked recessive inheritance. Genomic DNA was extracted from the third aborted male fetus and analyzed via trio whole-exome sequencing (WES). Total RNA was isolated from the pregnant woman to assess splicing variation at the mRNA level, and amniotic fluid was extracted from the woman for prenatal diagnosis on her fourth fetus.

Results: All four male fetuses were affected by severe hydrocephalus. We identified a maternally derived hemizygous splicing variation NM_000425.5:[c.3046+1G>A]; NP_000416.1 p.(Gly1016AspfsTer6) (chrX:153130275) in Intron 22 of the *L1CAM*. This variation disrupts the donor splice site and causes the retention of Intron 22, which results in frame shift and a premature termination codon at position 1021 with the ability to produce a truncated protein without the fifth fibronectin-repeat III, transmembrane, and cytoplasmic domains or to induce the degradation of mRNAs by nonsense-mediated mRNA decay. The same hemizygous variant was also detected in the amniocytes.

Conclusion: This report enhances our knowledge of genetic and phenotypic characteristics of X-linked fetal hydrocephalus, providing a new genetic basis for prenatal diagnosis and pre-implantation prenatal diagnosis.

KEYWORDS

fetal hydrocephalus, *L1CAM*, prenatal diagnosis, splicing variation

1 | INTRODUCTION

The human L1 cell adhesion molecule gene (*L1CAM*, OMIM "308840") is located on the X-chromosome at Xq28, spans 24,657 bp, and contains 28 exons (Li et al., 2020). The *L1CAM* gene is primarily expressed in the nervous system and encodes the L1 adhesion molecule protein, which is a transmembrane glycoprotein belonging to the immunoglobulin (Ig) superfamily. This protein is typically composed of a large extracellular region possessing six Ig-like and five fibronectin-repeat III (Fn III-like) domains, a single-pass transmembrane sequence, and a short intracellular cytoplasmic domain (Schäfer & Altevogt, 2010; Vos et al., 2010; Walmod, 2014). As a neuronal adhesion molecule, L1CAM mediates cell–cell adhesion, growth cone morphology, neurite outgrowth, myelination, axon bundling and pathfinding, long-term potentiation, neuronal cell survival and migration, and synaptogenesis (Schäfer & Altevogt, 2010; Vos et al., 2010; Walmod, 2014).

Pathogenic variants in *L1CAM* are associated with a wide spectrum of X-linked disorders summarized as the L1 syndrome (Stumpel & Vos, 2021). This syndrome comprises three clinical phenotypes: X-linked partial corpus callosum agenesis (CCA; OMIM 304100), hydrocephalus due to stenosis of the aqueduct of Sylvius (HSAS syndrome; OMIM 307000), and MASA syndrome (mental retardation, adducted thumbs, shuffling gait, and aphasia; OMIM 303350). As of March 2022, 325 variations have been reported in the *L1CAM* gene (http://www.hgmd.org): half of these are missense/nonsense mutations (52.0%), followed by small deletions (18.8%), splicing variants (18.2%), gross deletions (3.7%), small insertions (3.4%), small indels (1.5%), gross insertions (1.5%), and complex rearrangements (1.0%).

The present study reports a splicing variation in the *L1CAM* gene of a woman who experienced adverse pregnancy outcomes (thrice) due to severe cerebral ventricular enlargement of the fetus with an X-linked recessive mode of inheritance. She underwent prenatal diagnosis during her fourth pregnancy. The pathogenicity of this splicing variant was assessed at the mRNA level. We also analyzed the results of genetic analysis with respect to those of clinical examinations to confirm the diagnosis and prenatal diagnosis of recurrent fetal hydrocephalus.

2 | CASE PRESENTATION

2.1 | Clinical presentation

A 29-year-old pregnant woman, Gravida 4 Para 0, was referred to the medical genetics department and prenatal diagnosis center of the West China Second University Hospital because of recurrent fetal hydrocephalus (Figure 1a). The phenotypes of the woman and her partner were normal, their marriage was not consanguineous, and they denied a family history of genetic diseases. During the first and second pregnancies, severe fetal hydrocephalus was detected by fetal ultrasound imaging at 32 weeks and 28 weeks of gestation, respectively (Table 1). Therefore, the woman requested the termination of her pregnancies. Both fetuses were male according to the couple but this assessment was made without chromosomal or genetic analyses. The results of Down's screening (maternal serum screening) and TORCH in the two previous

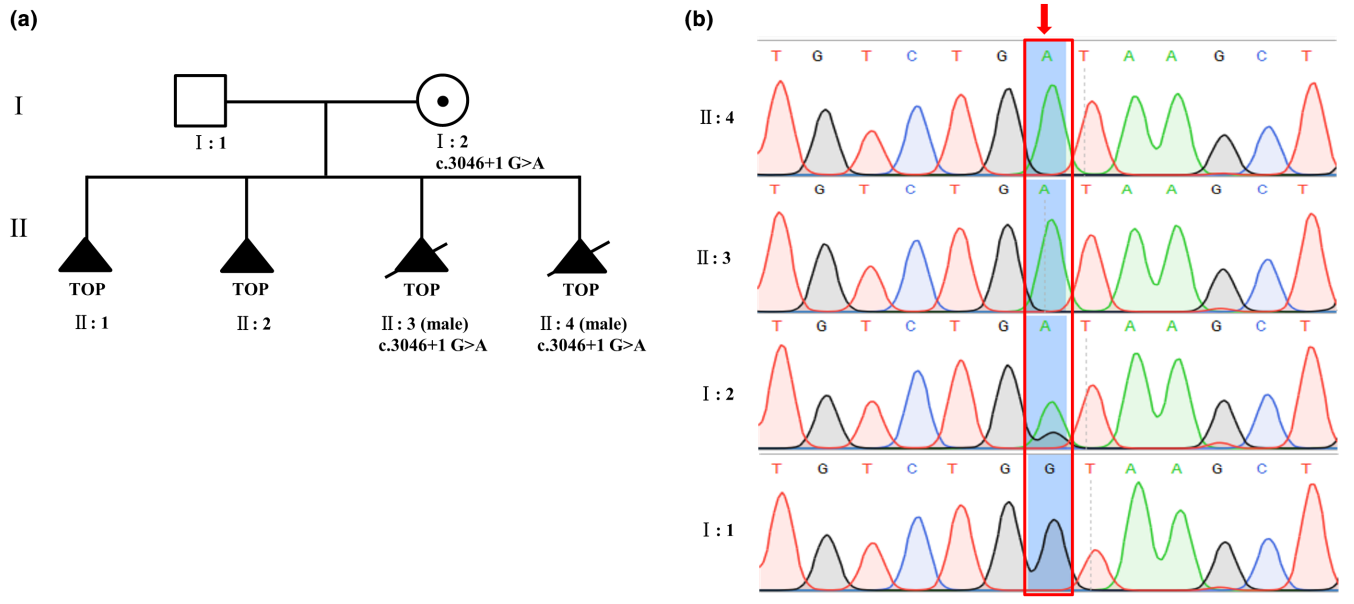

FIGURE 1 Pedigree of the family. (a) Four terminations of pregnancy in the family. TOP: termination of pregnancy. (b) Sanger sequencing analysis of II:4 (fetus), II:3 (fetus), I:2 (mother, carrier), and I:1 (father, wild type). The mutation is indicated by red arrows.

TABLE 1 Summary of prenatal characteristics and intrauterine outcome.

		US measure		MRI measure				Genetic testing			
Gravidity	Age (years)	GW (weeks)	Findings	GW (weeks)	Findings	Down's screening	Maternal TORCH	Karyotype	CNVs	SNVs	Intrauterine outcome
1	23	23+3 32	LVA/RVA(mm): <10 LVA/RVA(mm): 32/32 TVA(mm): 5 the transparent septum was absent			Low risk	Normal				TOP
2	25	23+3 26 28+1	RVA (mm): 10 LVA/RVA(mm): 23/26 LVA/RVA(mm): 31/31.5 thinned brain parenchyma, polyhydramnios			Low risk	Normal				TOP
3	28	23+4	LVA/RVA(mm): 16/17			Low risk	Normal	46,XY,16qh+	Negative	*L1CAM* c.3046+1G>A	TOP
4	29	21+3 23+3	LVA/RVA(mm): 11/10 LVA/RVA(mm): 14/18	23+5	LVA/RVA (mm): 16/16.2 corpus callosum agenesis	Low risk	Normal	46,XY		*L1CAM* c.3046+1G>A	TOP

Abbreviations: CNVs, copy number variants; GW, gestational weeks; MRI, magnetic resonance imaging; LVA, left ventricular atrium; RVA, right ventricular atrium; SNVs, single-nucleotide variations; TOP, termination of pregnancy; TORCH: toxoplasmosis, other (syphilis), rubella, cytomegalovirus, herpes simplex virus; TVA, the third ventricular atrium; US, ultrasound.

pregnancies were both normal. The karyotypes of the couple were normal (wife 46, XX, 16qh+, husband 46, XY).

Ultrasound examination during her third pregnancy also revealed severe hydrocephalus (left ventricle 16 mm, right ventricle 17 mm) in the fetus at 23 weeks and 4 days of gestation. Karyotype analysis from amniocytes revealed a normal karyotype (46, XY). Microdeletion/microduplication was excluded by copy-number variation sequencing (CNV-seq). The woman decided to terminate the pregnancy, and fetal tissues after the abortion were collected and sent for genetic analysis (II: 3).

While the trio-WES was being conducted, the woman became pregnant for the fourth time. A routine fetal ultrasound scan showed that the width of the lateral ventricles was 11 mm (left) and 10 mm (right) at 21 weeks and 3 days of gestation. Fetal ultrasonography was performed at 23 weeks and 3 days of gestation, revealing severe bilateral ventricular dilation (Figure 2a). The width of the left lateral ventricle was 14 mm and that of the right lateral ventricle was 18 mm, and the septum pellucidum was rather narrow (2 mm). These results were further confirmed by fetal magnetic resonance imaging (MRI), which revealed severe dilatation of the bilateral lateral ventricle (left 16 mm, right 16.2 mm) (Figure 2b) combined with the agenesis of the corpus callosum. Three parts (body, splenium, and rostrum) of the corpus callosum were not clearly visible (Figure 2c). Because same imaging results were obtained during previous pregnancies, amniotic fluid of the woman was collected (II: 4) and genetic testing was performed. A summary of prenatal characteristics and intrauterine outcomes is shown in Table 1.

2.2 | Genetic analysis

Trio WES was performed on fetal tissues from the third pregnancy to determine the potential genetic cause. We identified a maternally inherited hemizygous pathogenic variant, NM_000425.5:[c.3046+1G>A], in fetal tissues obtained after the abortion (II: 3), which was located in Intron 22 of the *L1CAM* gene. Subsequent Sanger sequencing confirmed that the fetus (II: 3) was hemizygous, the woman was heterozygous carrier (I: 2), and her partner was normal (I: 1) (Figure 1b).

All the three splice prediction algorithms revealed that the intronic c.3046+1G>A variation might influence mRNA splicing (Table S1). The cDNA amplicons showed two different bands: a longer abnormal band and a smaller wild-type band (Figure 3a). Sequencing of the longer product revealed the presence of a 116 bp intronic sequence adjacent to Exon 22 (r.3046_3047ins[ga;3046+1_3046+116]) (Figure 3c). The disruption of the donor splice site of Intron 22 inhibits splicing and results in the retention of Intron 22 in the aberrant transcript. A reading frame shift occurs at codon 1016, and the translation continues for five amino acids; finally, it is terminated early after reaching codon 1021 (NP_000416.1 p.Gly1016AspfsTer6) (Figure 3c). The fifth Fn III-like, transmembrane, and cytoplasmic domains are translated from codon 1017 to 1108, 1113 to 1143, and 1143 to 1257, respectively (http://www.l1cammutationdatabase.info) (Figure 4), the *L1CAM* variation may produce a truncated protein without these three domains or induce the degradation of mRNAs by nonsense-mediated mRNA decay (NMD).

After amplifying and sequencing the fragment around c.3046+1 on the DNA extracted from amniocytes (II: 4), the same hemizygous variant c.3046+1G>A was found (Figure 1b). The same transcription error was also detected in the current male fetus (Figure 3b).

According to the Criteria for classifying pathogenic variants of American College of Medical Genetics and Genomics Standards and Guidelines, this variant of *L1CAM* could be categorized as "pathogenic" with one pathogenic very strong evidence (PVS1): splicing, one pathogenic strong evidence (PS3): aberrant splicing was

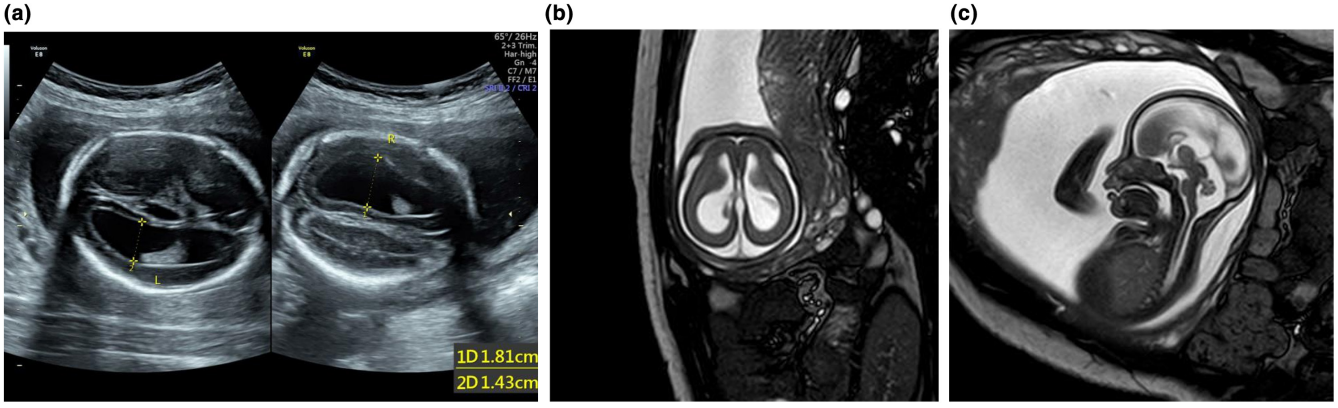

FIGURE 2 Imaging of the brain of II: 4 (fetus). Fetal ultrasound scan (a) and fetal MRI (b) showing dilated lateral ventricles. (c) Sagittal T2-weighted image showing corpus callosum agenesis at 23 weeks and 5 days of gestation.

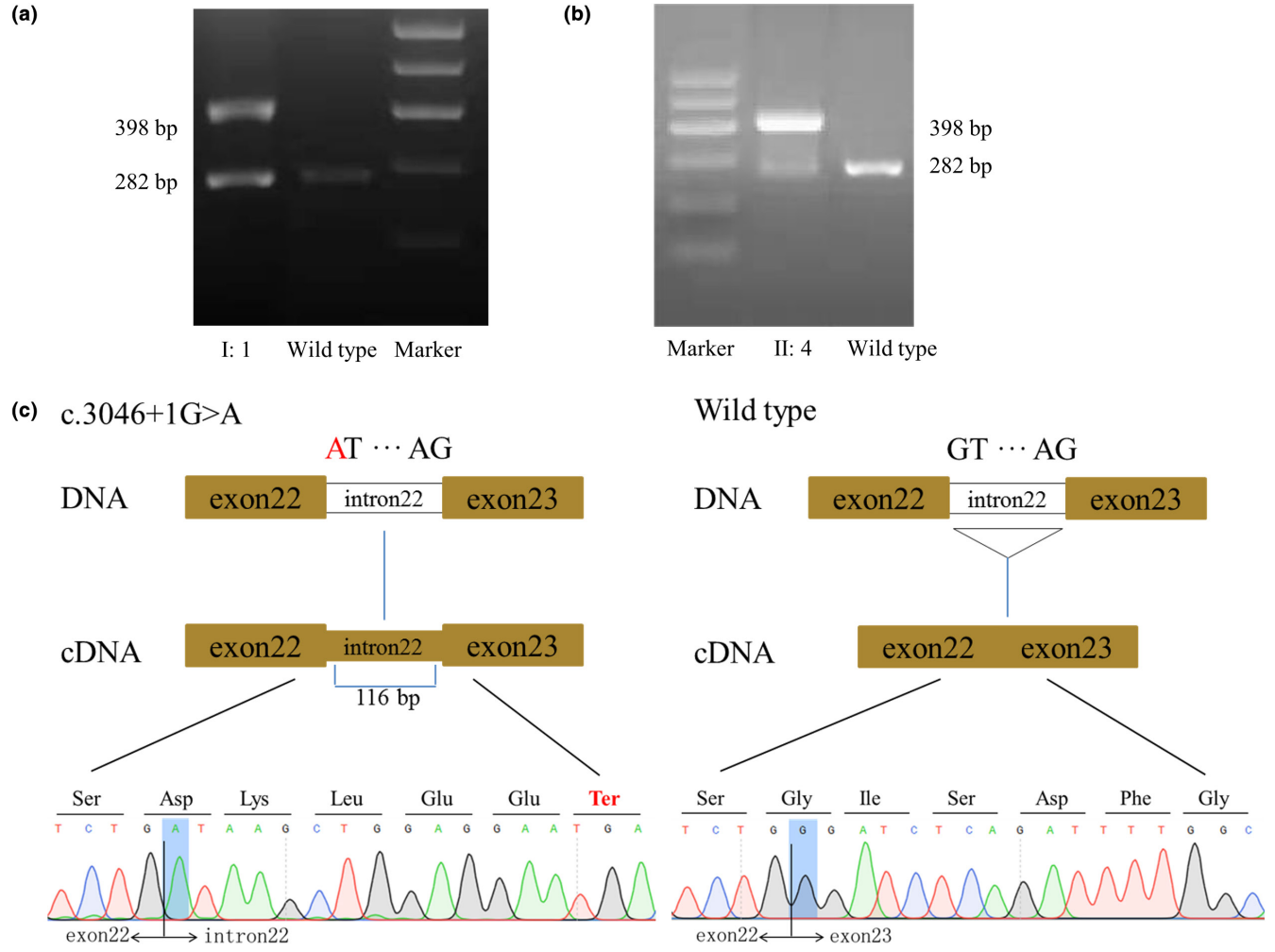

FIGURE 3 mRNA splicing analysis of c.3046 + 1 G > A in *LICAM*. In contrast to the control, two types of transcript (with and without Intron 22) were identified in the family members, I: 1 (a) and II: 4 (b). (c) Schematic representation of Exon 22, Intron 22, and Exon 23 organization in *L1CAM* and Sanger sequencing analysis of RT-PCR products.

showed by mRNA analysis, and one pathogenic moderate evidence (PM2): absent from controls in the general population databases and two pathogenic supporting evidence (PP1): cosegregation with disease in two affected family members in a gene definitively known to cause the disease and (PP4): patient's phenotype is highly specific for a disease with a single genetic etiology.

3 | MATERIALS AND METHODS

3.1 | Editorial policies and ethical considerations

This research was approved by the Medical Ethics Committee of the West China Second University Hospital, Sichuan University (approval No. [2021] 157). Informed consent forms were signed by all subjects.

3.2 | Clinical material

Blood samples were obtained from the pregnant woman and her partner, fetal tissue samples were obtained from the third aborted fetus of the woman, and amniotic fluid samples were obtained during the fourth pregnancy. Genomic DNA was isolated from all samples using QIAamp DNA Blood Mini Kit (Qiagen, Valencia, CA, USA) according to the manufacturer's instructions. Total RNA was isolated from the peripheral blood and amniocytes using the RNApure Blood Kit (CWBIO, Beijing, China).

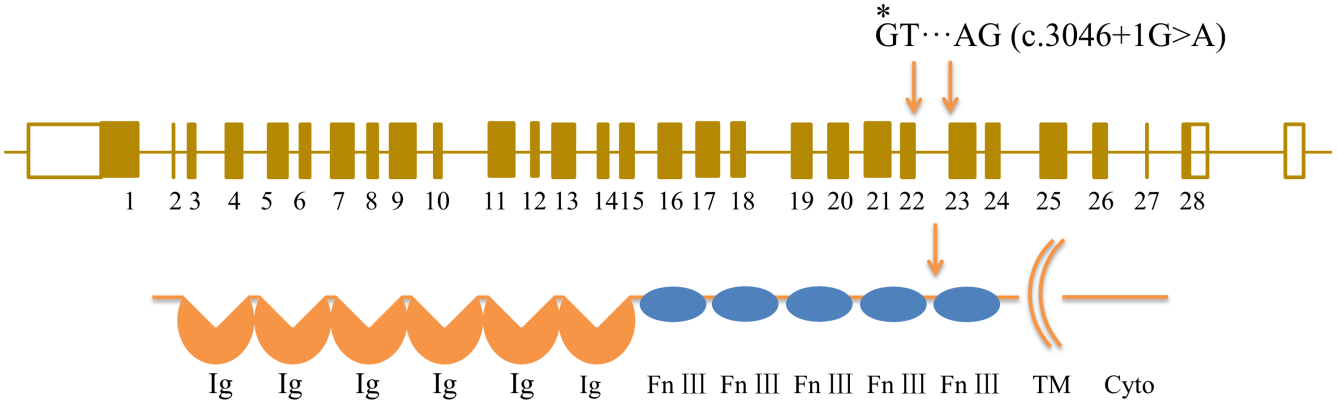

Protein domain	Ig-like	Ig-like	Ig-like	Ig-like	Ig-like	Ig-like	Fn III-like	Fn III-like	Fn III-like	Fn III-like	Fn III-like	Tranme-nbrane	Cytopl-asmic
Amino acid	33-133	134-230	238-330	331-422	423-515	516-609	612-710	714-808	812-904	918-1012	1017-1108	1113-1143	1143-1257

FIGURE 4 Genomic organization of human *L1CAM* gene and the domain structure of the L1CAM protein. The mutation identified in L1CAM is indicated by *.

3.3 | Variant identification and characterization

Whole-exome capture was conducted by IDT's xGen Exome Research Panel (Integrated DNA Technologies, Skokie, IL, USA) according to standard methods. Sequencing was performed on the Illumina NavoSeq6000 platform (Illumina, San Diego, CA, USA) with 150-bp paired-end reads. The mean depth of coverage of the sequenced samples was 100 ×. Sequencing data were aligned to the human reference genome (hg19/GRCh37) using the Burrows-Wheeler Aligner tool (BWA, http://bio-bwa.sourceforge.net/). Variations were identified using Berry Genomics and GATK software (https://software.broadinstitute.org/gatk/). Detected variants were annotated and filtered using ANNOVAR software (http://annovar.openbioinformatics.org/en/latest/) and associated with population databases 1000 Genome Project (http://browser.1000genomes.org) and GnomAD Aggregation Database (http://gnomad.broadinstitute.org/). Variations registered with minor allele frequency (MAF) ≥ 1% for a recessive inheritance model or ≥0.1% for a dominant inheritance model were excluded. Impact of variants on splicing was predicted by different splice prediction algorithms: dpsi_zscore using the recommended threshold of 2, dbscSNV_ADA_ SCORE using the recommended threshold of 0.6 and SpliceAI using the recommended threshold of 0.5. Clinical significance of variants was evaluated based on the published literatures and disease databases: PubMed (https://www.ncbi.nlm.nih.gov/pubmed/), ClinVar (http://www.ncbi.nlm.nih.gov/clinvar), OMIM (http://www.omim.org), Human Gene Mutation Database (HGMD, http://www.hgmd.org), and Human Genome Variation Society (http://www.hgvs.org/dblist/dblist.html). Variants were classified according to five categories, pathogenic, likely pathogenic, uncertain significance, likely benign, and benign, according to the American College of Medical Genetics and Genomics (ACMG) guidelines (Richards et al., 2015). The potential pathogenic variants were validated using Sanger sequencing on an ABI 3500 genetic analyzer (Applied Biosystems, Waltham, MA, USA). Nucleotide sequence variant data have been submitted to ClinVar (Variation ID: 1344539).

3.4 | mRNA splicing analysis

To confirm the predicted splicing defect of the mutated *L1CAM* mRNA, mRNA splicing analysis was performed using peripheral blood sample of the pregnant woman. After total RNA extraction, RT-PCR was performed using the HiFiScript cDNA synthesis kit (CWBIO, Beijing, China) according to the manufacturer's instructions. The target regions of the cDNA sequence around the c.3046 + 1G > A mutation of *L1CAM* (Exons 22–24) were amplified by PCR using 2×TSINGKE master mix (Tsingke, Beijing). The primer sequences used for PCR were as follows: E22F: 5′—ACAACCTGACCGATCTCAGC—3′ (sense) and E24R: 5′—GGTTGTAGCTGACATACTGTGG—3′ (antisense) (Tsingke, Beijing, China). The PCR products

were run on 2% agarose gel electrophoresis and verified by Sanger sequencing.

3.5 | Chromosomal microarray analysis and chromosomal karyotype analysis

Chromosomal microarray analysis and chromosomal karyotype analysis were performed as previously described (Hu et al., 2019).

4 | DISCUSSION

The etiology of fetal hydrocephalus is complicated and could be related to chromosomal abnormalities, copy-number variants, monogenic disorders, intrauterine infection, or intraventricular hemorrhage (Wang et al., 2021). Among these causes, genetic causes account for 40% of cases, and the most common heritable form is X-linked hydrocephalus due to *L1CAM* (Varela et al., 2020). Variations in *L1CAM* lead to a wide phenotypic spectrum, with neuropathological manifestations in affected fetuses, including hydrocephalus, corpus callosum abnormalities, aqueductal stenosis, corticospinal tract abnormalities, and adducted thumbs (Adle-Biassette et al., 2013). In this study, we identified a splicing variation in *L1CAM*, likely responsible for recurrent fetal hydrocephalus. All four male fetuses were affected by severe hydrocephalus, mild ventriculomegaly was observed at around 23 weeks of gestation, and the severity of lateral ventricular dilation significantly increased with the gestational age. The width of the lateral ventricle expanded from 10 mm to about 26 mm by 3 weeks of gestation and progressed to hydranencephaly after 5 weeks of gestation (II: 2). Except for symmetric dilatation of the lateral ventricle, the dilatation of the third ventricle and the absence of septum pellucidum were found in the first fetus (II: 1), thinned brain parenchyma and polyhydramnios in the third fetus (II: 2), and partial agenesis of the corpus callosum detected by MRI in the fourth fetus (II: 4). Previous studies have also reported these intrauterine manifestations in fetuses with a family history of X-linked hydrocephalus (Accogli et al., 2021; Ferese et al., 2016; Guo et al., 2020; Sun et al., 2019), further establishing the correlation between *L1CAM* and recurrent fetal hydrocephalus.

L1CAM protein coordinates multiple adhesion and signaling events in nervous system development, maintenance, and function. The Ig-like domains play a major role in heterophilic interactions and homophilic interactions through binding a number of glycoproteins including themselves at the cell surface (Schäfer & Altevogt, 2010; Walmod, 2014). These cooperative interactions are crucial for proper adhesion and functioning of L1CAM. The Fn III-like domains directly interact with the immunoglobulin modules of fibroblast growth factor receptor 1 (FGFR1), and this interaction plays an important role in modulating neuronal differentiation (Samatov et al., 2016; Walmod, 2014). The cytoplasmic domain mediates linkage to the actin cytoskeleton and the endosomal membrane system by interacting with a variety of intracellular proteins such as kinases and adaptor molecules, thus enabling axonal targeting, stabilization at the cell surface and cell-surface expression (Grońska-Pęski et al., 2020; Schäfer & Frotscher, 2012; Tai et al., 2019). Loss-of-function mutations in *L1CAM* would destroy the adhesion and signaling events of neuronal cells during brain development.

The *L1CAM* variant c.3046 + 1G > A identified in this study has not been previously described. Although the *L1CAM* variant c.3046 + 1G > C was reported in ClinVar (rs1557090220), but the effect of sequence change on RNA splicing has not been confirmed by transcriptional studies. Splicing mutations can result in complete skipping of exon, retention of intron, or introduction of a new splice site within an exon or intron (Baralle & Baralle, 2005). Actually, the variant displays the retention of Intron 22: a donor splice site is disrupted within Exon 22 of the gene and leads to the incorporation of additional 116 nucleotides between Exons 22 and 23. Consequently, a reading frame shift occurs at codon 1016 and produces a premature stop codon at position 1021. We proposed the possible pathogenesis inducing fetal hydrocephalus in the family are: (1) the novel mutation is located at the fifth Fn III-like domain, which results in a premature stop codon may produce a truncated L1CAM protein without the fifth Fn III-like, transmembrane, and intracellular cytoplasmic domains. The absence of these domains leads to the loss function of L1CAM protein. (2) The premature termination codon at position 1021 may lead to the degradation of mRNAs by NMD. Further studies would be needed to verify the predicted effect of this variation on L1CAM structure and function.

In this study, we have identified a novel variation which adjacent to a previously reported splice site variant (c.3047–1 G > A), as documented in the literature. Two brothers carrying the c. 3047–1 G > A variation were diagnosed as L1 syndrome after birth, and both presented with severe ventricular dilation, rippled ventricular wall, adducted thumb, and spastic paraplegia. The elder brother died at 6 years of age (Kanemura et al., 2006). Regretfully, the clinical parameters in utero were not collected. To date, about 56 splicing mutations in *L1CAM* gene have been reported in HGMD: several studies have described the prenatal features associated with splicing mutations (Isik et al., 2018; Okamoto

et al., 2004; Rehnberg et al., 2011; Serikawa et al., 2014; Sun et al., 2019). Among them, intrauterine hydrocephalus is the basic characteristic, it occurs at different gestations from 17 weeks to 36 weeks. Agenesis of the corpus callosum would be discovered if MRI examination was performed (Ferese et al., 2016; Okamoto et al., 2004; Serikawa et al., 2014; Sun et al., 2019). Other sporadic features like lissencephaly (Ferese et al., 2016), a hypoplastic cerebellum (Serikawa et al., 2014), and a thinned cortex (Okamoto et al., 2004) were also found. In this study, although four male fetuses have hydrocephalus, while the other phenotype are difference, such as the absent septum pellucidum was found in the first fetus, thinned brain parenchyma and polyhydramnios in the third fetus, and partial agenesis of the corpus callosum was detected by MRI in the fourth fetus. To some extent intrauterine phenotype is limited, as it depend mainly on imaging methods, and molecular testing is particularly important for prenatal diagnosis. Performing trio-WES prenatally is an option but it is time consuming and expensive. On the other hand, the possible detection rate of *L1CAM* variation in a family of more than two affected individuals and more than one typical phenotypic finding is 93% (Finckh et al., 2000). Thus *L1CAM* gene sequencing is recommend as a routine examination in the prenatal diagnosis of X-linked recurrent fetal hydrocephalus.

In conclusion, we identified a novel splicing variation c.3046 + 1G > A in *L1CAM* in a healthy pregnant woman who had multiple adverse pregnancy outcomes due to cerebral ventricular enlargement with an X-linked recessive mode of inheritance. This variation results in a premature stop codon that may produce an aberrant truncated protein which lacks one Fn III-like domain, a transmembrane segment, and a C-terminal cytoplasmic sequence or leads to the degradation of mRNAs by NMD. Our report enhances the understanding of genetic and phenotypic characteristics of X-linked fetal hydrocephalus and provides a new genetic basis for prenatal diagnosis and pre-implantation prenatal diagnosis of this disorder.

AUTHOR CONTRIBUTIONS

TH and XMZ designed the study and drafted the manuscript. QY and JNJ collected the samples and clinical data. TH and LKX conducted the experiments. BCX, MY, and QQX conducted the genetic data interpretation. XMZ, SLL, and HW conceived and supervised the study and revised the manuscript. All authors have read and approved the final manuscript.

ACKNOWLEDGMENTS

We thank all contributors in this study.

FUNDING INFORMATION

This work was supported by a grant from the Science and Technology Department of the Sichuan Province of China (grant number: 2017SZ0111) and the New Bud Fund of West China Second Hospital of Sichuan University (grant number: KX240).

CONFLICT OF INTEREST STATEMENT

The authors declare that they have no competing interests.

DATA AVAILABILITY STATEMENT

The datasets used or analyzed during the current study are available from the corresponding author on reasonable request.

ORCID

Tiantian He https://orcid.org/0000-0002-6855-6545

REFERENCES

Accogli, A., Goergen, S., Izzo, G., Mankad, K., Krajden Haratz, K., Parazzini, C., Fahey, M., Menzies, L., Baptista, J., Carpineta, L., Tortora, D., Fulcheri, E., Gaetano Vellone, V., Paladini, D., Spaccini, L., Toto, V., Trayers, C., Ben Sira, L., Reches, A., ... Severino, M. (2021). L1CAM variants cause two distinct imaging phenotypes on fetal MRI. *Annals of Clinical Translational Neurology*, *8*(10), 2004–2012. https://doi.org/10.1002/acn3.51448

Adle-Biassette, H., Saugier-Veber, P., Fallet-Bianco, C., Delezoide, A. L., Razavi, F., Drouot, N., Bazin, A., Beaufrère, A. M., Bessières, B., Blesson, S., Bucourt, M., Carles, D., Devisme, L., Dijoud, F., Fabre, B., Fernandez, C., Gaillard, D., Gonzales, M., Jossic, F., ... Laquerrière, A. (2013). Neuropathological review of 138 cases genetically tested for X-linked hydrocephalus: Evidence for closely related clinical entities of unknown molecular bases. *Acta Neuropathologica*, *126*(3), 427–442. https://doi.org/10.1007/s00401-013-1146-1

Baralle, D., & Baralle, M. (2005). Splicing in action: Assessing disease causing sequence changes. *Journal of Medical Genetics*, *42*(10), 737–748. https://doi.org/10.1136/jmg.2004.029538

Ferese, R., Zampatti, S., Griguoli, A. M., Fornai, F., Giardina, E., Barrano, G., Albano, V., Campopiano, R., Scala, S., Novelli, G., & Gambardella, S. (2016). A new splicing mutation in the L1CAM gene responsible for X-linked hydrocephalus (HSAS). *Journal of Molecular Neuroscience*, *59*(3), 376–381. https://doi.org/10.1007/s12031-016-0754-3

Finckh, U., Schröder, J., Ressler, B., Veske, A., & Gal, A. (2000). Spectrum and detection rate of L1CAM mutations in isolated and familial cases with clinically suspected L1-disease. *American Journal of Medical Genetics*, *92*(1), 40–46.

Grońska-Pęski, M., Schachner, M., & Hébert, J. M. (2020). L1cam curbs the differentiation of adult-born hippocampal neurons. *Stem Cell Research*, *48*, 101999. https://doi.org/10.1016/j.scr.2020.101999

Guo, D., Shi, Y., Jian, W., Fu, Y., Yang, H., Guo, M., ... Yao, R. (2020). A novel nonsense mutation in the L1CAM gene responsible for X-linked congenital hydrocephalus. *The Journal of Gene Medicine*, *22*(7), e3180. https://doi.org/10.1002/jgm.3180

Hu, T., Zhang, Z., Wang, J., Li, Q., Zhu, H., Lai, Y., ... Liu, S. (2019). Prenatal diagnosis of chromosomal aberrations by chromosomal microarray analysis in fetuses with ultrasound anomalies in the urinary system. *Prenatal Diagnosis*, *39*(12), 1096–1106. https://doi.org/10.1002/pd.5550

Isik, E., Onay, H., Atik, T., Akgun, B., Cogulu, O., & Ozkinay, F. (2018). Clinical and genetic features of L1 syndrome patients: Definition of two novel mutations. *Clinical Neurology and Neurosurgery*, *172*, 20–23. https://doi.org/10.1016/j.clineuro.2018.06.007

Kanemura, Y., Okamoto, N., Sakamoto, H., Shofuda, T., Kamiguchi, H., & Yamasaki, M. (2006). Molecular mechanisms and neuroimaging criteria for severe L1 syndrome with X-linked hydrocephalus. *Journal of Neurosurgery*, *105*(5 Suppl), 403–412. https://doi.org/10.3171/ped.2006.105.5.403

Li, Y. T., Chen, J. S., Jian, W., He, Y. D., Li, N., Xie, Y. N., Wang, J., Zhang, V. W., Huang, W. R., Jiang, F. M., Ye, X. Q., Chen, D. J., & Chen, M. (2020). L1CAM mutations in three fetuses diagnosed by medical exome sequencing. *Taiwanese Journal of Obstetrics & Gynecology*, *59*(3), 451–455. https://doi.org/10.1016/j.tjog.2020.03.022

Okamoto, N., Del Maestro, R., Valero, R., Monros, E., Poo, P., Kanemura, Y., & Yamasaki, M. (2004). Hydrocephalus and Hirschsprung's disease with a mutation of L1CAM. *Journal of Human Genetics*, *49*(6), 334–337. https://doi.org/10.1007/s10038-004-0153-4

Rehnberg, M., Jonasson, J., & Gunnarsson, C. (2011). Novel L1CAM splice site mutation in a young male with L1 syndrome. *American Journal of Medical Genetics. Part A*, *155a*(2), 439–441. https://doi.org/10.1002/ajmg.a.33803

Richards, S., Aziz, N., Bale, S., Bick, D., das, S., Gastier-Foster, J., Grody, W. W., Hegde, M., Lyon, E., Spector, E., Voelkerding, K., Rehm, H. L., & ACMG Laboratory Quality Assurance Committee. (2015). Standards and guidelines for the interpretation of sequence variants: A joint consensus recommendation of the American College of Medical Genetics and Genomics and the Association for Molecular Pathology. *Genetics in Medicine*, *17*(5), 405–424. https://doi.org/10.1038/gim.2015.30

Samatov, T. R., Wicklein, D., & Tonevitsky, A. G. (2016). L1CAM: Cell adhesion and more. *Progress in Histochemistry and Cytochemistry*, *51*(2), 25–32. https://doi.org/10.1016/j.proghi.2016.05.001

Schäfer, M. K., & Altevogt, P. (2010). L1CAM malfunction in the nervous system and human carcinomas. *Cellular and Molecular Life Sciences*, *67*(14), 2425–2437. https://doi.org/10.1007/s00018-010-0339-1

Schäfer, M. K., & Frotscher, M. (2012). Role of L1CAM for axon sprouting and branching. *Cell and Tissue Research*, *349*(1), 39–48. https://doi.org/10.1007/s00441-012-1345-4

Serikawa, T., Nishiyama, K., Tohyama, J., Tazawa, R., Goto, K., Kuriyama, Y., Haino, K., Kanemura, Y., Yamasaki, M., Nakata, K., Takakuwa, K., & Enomoto, T. (2014). Prenatal molecular diagnosis of X-linked hydrocephalus via a silent C924T mutation in the L1CAM gene. *Congenital Anomalies*, *54*(4), 243–245. https://doi.org/10.1111/cga.12069

Stumpel, C., & Vos, Y. J. (2021). L1 Syndrome. In M. P. Adam, H. H. Ardinger, R. A. Pagon, S. E. Wallace, L. J. H. Bean, G. Mirzaa, & A. Amemiya (Eds.), *GeneReviews(®)*. University of Washington, Seattle.

Sun, Y., Li, Y., Chen, M., Luo, Y., Qian, Y., Yang, Y., Lu, H., Lou, F., & Dong, M. (2019). A novel silent mutation in the L1CAM gene causing fetal hydrocephalus detected by whole-exome sequencing. *Frontiers in Genetics*, *10*, 817. https://doi.org/10.3389/fgene.2019.00817

Tai, Y., Gallo, N. B., Wang, M., Yu, J. R., & Van Aelst, L. (2019). Axo-axonic innervation of neocortical pyramidal neurons by GABAergic chandelier cells requires AnkyrinG-associated L1CAM. *Neuron*, *102*(2), 358–372.e359. https://doi.org/10.1016/j.neuron.2019.02.009

Varela, M. F., Miyabe, M. M., & Oria, M. (2020). Fetal brain damage in congenital hydrocephalus. *Child's Nervous System*, *36*(8), 1661–1668. https://doi.org/10.1007/s00381-020-04657-9

Vos, Y. J., de Walle, H. E., Bos, K. K., Stegeman, J. A., ten Berge, A., Bruining, M., van Maarle, M., Elting, M. W., den Hollander, N., Hamel, B., Fortuna, A. M., Sunde, L. E., Stolte-Dijkstra, I., Schrander-Stumpel, C. T., & Hofstra, R. M. (2010). Genotype-phenotype correlations in L1 syndrome: A guide for genetic counselling and mutation analysis. *Journal of Medical Genetics*, *47*(3), 169–175. https://doi.org/10.1136/jmg.2009.071688

Walmod, P. S. (2014). Introduction. Cell adhesion molecules: Implications in neurological diseases. *Advances in Neurobiology*, *8*, xvii–xxi.

Wang, R., Ding, Y., Yang, M., & Lai, W. (2021). Diagnosis, management, and neurodevelopmental outcomes of fetal hydrocephalus: An observational prospective study. *Child's Nervous System*, *37*, 3777–3784. https://doi.org/10.1007/s00381-021-05213-9

SUPPORTING INFORMATION

Additional supporting information can be found online in the Supporting Information section at the end of this article.

How to cite this article: He, T., Yao, Q., Xu, B., Yang, M., Jiang, J., Xiang, Q., Xiao, L., Liu, S., Wang, H., & Zhang, X. (2023). A novel splicing variation in *L1CAM* is responsible for recurrent fetal hydrocephalus. *Molecular Genetics & Genomic Medicine*, *11*, e2253. https://doi.org/10.1002/mgg3.2253